NHC-Catalyzed Homoenolate Reaction of Enals and Nitroalkenes: Computational Study of Mechanism, Chemoselectivity and Stereoselectivity

Journal:	*Organic Chemistry Frontiers*
Manuscript ID:	QO-RES-02-2014-000036.R1
Article Type:	Research Article
Date Submitted by the Author:	02-Apr-2014
Complete List of Authors:	Zhang, Qi; University of Science & Technology of China, Yu, Haizhu; University of Science & Technology of China, Fu, Yao; University of Science & Technology of China, Department of Chemistry

Cite this: DOI: 10.1039/c0xx00000x

www.rsc.org/xxxxxx

ARTICLE TYPE

NHC-Catalyzed Homoenolate Reaction of Enals and Nitroalkenes: Computational Study of Mechanism, Chemoselectivity and Stereoselectivity

Qi Zhang,[a] Hai-Zhu Yu[b] and Yao Fu*[a]

Received (in XXX, XXX) Xth XXXXXXXXX 20XX, Accepted Xth XXXXXXXXX 20XX
DOI: 10.1039/b000000x

A systematic theoretical study has been carried out on the NHC-catalyzed homoenolate reaction of enals and nitroalkenes. The detailed mechanism of these nitroalkenes participated homoenolate reactions, the chemoselectivity of homoenolate (vs Stetter) pathway and the intriguing *syn*- (vs *anti*-) stereoselectivity have been investigated. Calculations show that the homoenolate and Stetter reaction (Path-homo and Path-set) first undergo the same formation process of Breslow intermediate, which proceeds via HOAc mediated stepwise mechanism. Subsequent process of Path-homo consists of five steps: nucleophilic attack of Breslow intermediate (C3 atom) to nitroalkene, intramolecular proton transfer, HOAc involved protonation of C2, concerted nucleophilic attack of OEt to carbonyl, and final carbene dissociation. Subsequent process of Path-set consists of three steps: nucleophilic attack of Breslow intermediate (C1 atom) to nitroalkene, intramolecular proton transfer and carbene dissociation. Path-homo is more feasible than Path-set. The highly exergonic nucleophilic attack, the facile intramolecular proton transfer and attack of OEt to carbonyl in Path-homo result in its feasibility. The stereoselectivity determining step of Path-homo is the attack of Breslow intermediate to the nitroalkene, in which the steric hindrance and hydrogen bonding determine the *syn* stereoselectivity.

1. Introduction

N-heterocyclic carbenes (NHCs) catalyzed umpolung reactions have made rapid progress in the past few decades.[1] Among these, NHCs are traditionally used as acyl anion equivalents (d^1-nucleophile) to participate in Stetter,[1c,2] benzoin,[3] redox[4] and other reactions[5]. When the reaction substrates are enals, NHCs can also be used as homoenolate equivalents (d^3-nucleophile), to participate in the homoenolate reactions (eq 1 in Scheme 1).[1b,6] In 2004, Bode[7a] and Glorius[8] et al. reported the pioneering studies on NHCs catalyzed homoenolate reactions. The nucleophilic homoenolate intermediates generated in these processes further reacted with the electrophilic substrates (aldehydes) to synthesize γ-lactones. This breakthrough discovery turns α, β unsaturated aldehydes into d^3-nucleophiles, thus provides a new catalytic method for carbon-carbon bond building. In addition to Bode[7] and Glorius[8] groups, Nair,[9] Scheidt,[10] Liu,[11] and Rovis[12] et al. have also made outstanding contributions in homoenolate reactions with a variety of active electrophiles to obtain heterocyclic compounds such as cis-γ-lactam, γ-butyrolactone and cyclopentene. In addition to cyclic compounds, non-cyclic compounds can also be obtained from homoenolate reactions. One of the most important non-cyclization homoenolate reactions involves the nitroalkenes as electrophiles.

In 2009, Nair[9c] group reported the imidazolinium precatalyst-catalyzed homoenolate reaction between aryl nitroalkenes and enals, and obtained *anti*-δ-nitro esters (eq 2); Similarly, Liu et al.

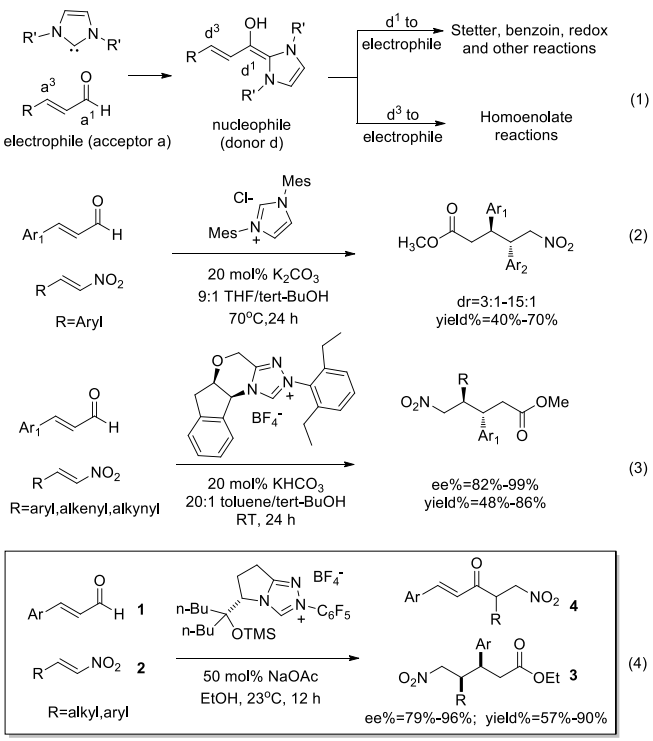

Scheme 1

Cite this: DOI: 10.1039/c0xx00000x

www.rsc.org/xxxxxx

ARTICLE TYPE

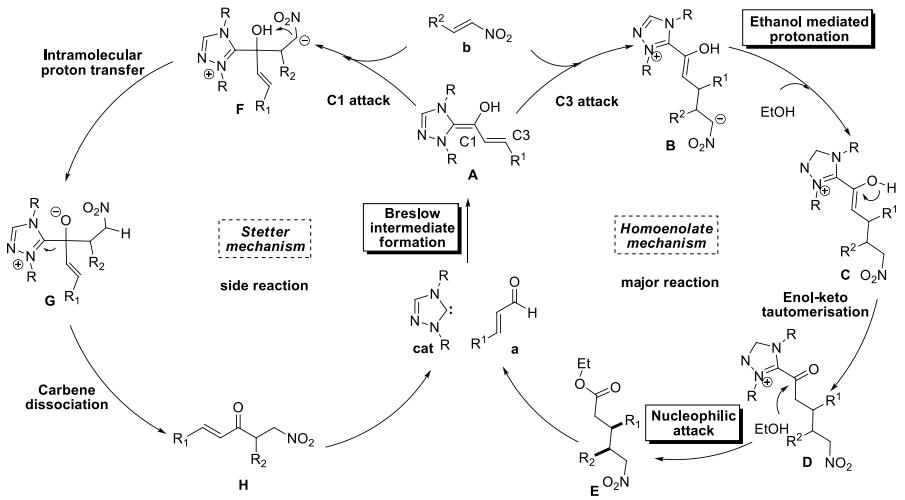

Scheme 2 Proposed mechanism of homoenolate and Stetter reaction

recently[11] reported the triazolium salts precatalyst-catalyzed homoenolate reaction between aryl/alkenyl/alkynyl nitroalkenes and enals, and obtained *anti*-δ-nitro ester (eq 3); Very recently, Rovis[12a] group exploited the homoenolate reaction between alkyl/aryl substituted nitroalkenes and enals, unexpectedly obtained the *syn* configuration product **3** accompanied with trace amount of Stetter product **4** (eq 4).

Despite of the great progress of the nitroalkenes electrophiles participated non-cyclization homoenolate reactions, the detailed mechanism of them remains unclear. Take eq 4 as an example, Nair[9c] et al. proposed that the substrate first transforms to the Breslow intermediate **A**; then the C3 atom of **A** attacks the nitroalkene to obtain **B**, followed by ethanol mediated protonation, enol-keto tautomerisation, and a final nucleophilic attack of the ethanol to carbonyl to yield the non-cyclization product **E** (Scheme 2). The above homoenolate process is favored than side reaction (Stetter) process. In Stetter reaction, C1 atom of intermediate **A** attacks nitroalkene, then the intramolecular proton transfer occurs in molecule **F** to give **G**, and the formation of the product **H** can be finally achieved by the carbene dissociation step.[13] Nonetheless, two problems remain to be settled in the aforementioned mechanisms. First, the details for the NHC catalyzed formation of Breslow intermediate are under debate. As shown in Scheme 3a, two types of mechanisms, i.e. the mechanisms in absence of conjugated acid and the mechanisms with the aid of conjugated acid might occur. For the first type, the direct 1,2 migration mechanism[14] (Path-a), the intermolecular proton transfer mechanism[15] (Path-b) between two NHC/benzaldehyde coupled intermediates, and the carbene ring on NHC involved indirect proton transfer mechanism[16] (Path-c) have all been previously proposed computationally. Experimentally, Rovis et al.[13a] envisioned that the proton is shuttled by the aryl ring on NHC catalyst (Path-d). For the second type, both the concerted proton transfer mechanism involving five-[17,18] or seven-membered[2b] ring transition state (Path-e) and the stepwise proton transfer mechanism[19] (Path-f) might occur. Currently, it remains unknown which mechanism (Paths a-f in Scheme 3a) is the most favored. Meanwhile, the subsequent steps from the Breslow intermediate in homoenolate reaction mechanism are desired to be examined, because the weak acid (HOEt) mediated protonation[20] of intermediate **B** and the nucleophic attack of **D** might be very difficult (Scheme 3b). In this context, we speculate that the intermediate **B** may undergo an alternative mechanism to generate the homoenolate product.

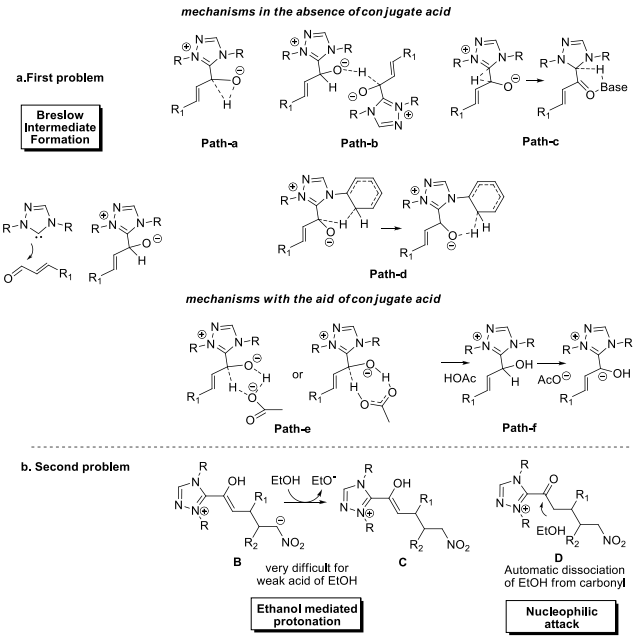

Scheme 3 Two unsettled mechanistic problems

Cite this: DOI: 10.1039/c0xx00000x

www.rsc.org/xxxxxx

ARTICLE TYPE

In order to solve the above mechanistic problems, we carried out theoretical calculations on the mechanism of nitroalkene participated homoenolate reaction. Meanwhile, the origin of the chemoselectivity of homoenolate (vs Stetter) reaction and the stereoselectivity of the intriguing *syn*- (vs *anti*-) homoenolate reaction shown in eq 4 has also been investigated. According to our calculations, the Breslow intermediate is generated through Path-f (conjugate acid involved stepwise proton transfer), rather than the direct proton transfer (Path-a), coupled intermediate (Path-b), carbene ring on NHC catalyst involved indirect proton transfer (Path-c), aryl ring on NHC catalyst involved proton transfer (Path-d) or conjugate acid involved concerted proton transfer mechanism (Path-e). As to the subsequent steps in homoenolate reaction (Path-homo), the Breslow intermediate first undergoes the nucleophilic attack of C3 atom to nitroalkene, and the formed intermediate (**B**, Scheme 2) then experiences the intramolecular protonation by hydroxy group (instead of the ethanol mediated intermolecular protonation). After the subsequent enol-keto tautomerisation, the formed intermediate (**D**) is attacked by a forming OEt^- of HOEt (instead of direct attack of HOEt). Finally, the product is obtained after the dissociation of carbene. The proposed mechanism is slightly different from that shown in Scheme 2 in the intramolecular protonation and attack of OEt^- to the carbonyl steps. The proposed mechanism has been verified by the good consistency between the calculation results and the experiments on the observed chemo- and stereoselectivity. Analyzing the reason for selectivity, we found that the two facile steps (the intramolecular protonation and attack of ^-OEt to the carbonyl steps) in Path-homo result in the feasibility of homoenolate reaction (over the Stetter reaction). Meanwhile, the stereoselective determining step of Path-homo is the attack of Breslow intermediate (**A)** to the nitroalkene. In this step, the steric hindrance between ethyl of the nitroalkene and alkyl substituent on the carbene ring, and hydrogen bonding between the nitro of the nitroalkene and the hydroxy group determine the stereoselectivity.

2. Computational methods and model reaction

2.1 Computational methods

Gaussian09 suite of program[21] was used for calculations in this study. The B3LYP[13b,13c,15,17,18,22,23] method combined with the 6-31+G(d) basis set was used for unrestricted geometry optimization in ethanol solvent (consistent with Rovis's experiments[12a], with SMD[24,25] model) on all structures. To get the thermodynamic corrections of Gibbs free energy and verify the stationary points to be local minima or saddle points, we conducted frequency analysis at the same level with optimization. For all transition states, we performed the intrinsic reaction coordinate (IRC) analysis to confirm that they connect the correct reactants and products on the potential energy surfaces.[26] For compounds that may have different conformations, various structures were calculated and the lowest energy conformation is used in the following discussions.

M06[27,28]/6-31+G(d,p) method with the SMD[24,25] model was used for the solution phase single-point energy calculations of all these stationary points (ethanol is used as solvent). All energetics involved in this study are calculated by adding the Gibbs free energy correction calculated at B3LYP/6-31G(d) and the single-point energy calculated at the M06/6-31+G(d,p) method.[28]

2.2 Model Reaction

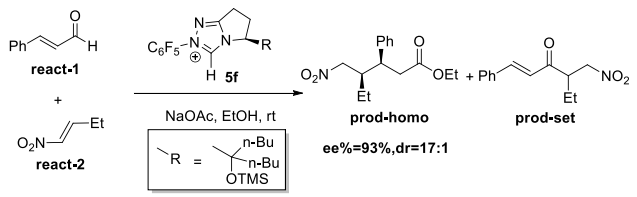

Scheme 4 Model reaction used in calculation

In the present study, the homoenolate and Stetter reactions of enal **react-1** and nitroalkene **react-2** in producing the (3S, 4R) configuration product **prod-homo** and the byproduct **prod-set** were chosen as the model reactions (Scheme 4).[12a] Consistent with Rovis's experiment, NHC catalyst **5f**, HOEt and NaOAc were chosen as the catalyst, solvent, and base, respectively.[12a] Mechanisms of homoenolate and Stetter reactions are named as Path-homo and Path-set respectively. In Rovis' experiment, the ratio of the yield of homoenolate and Stetter product is higher than 20:1, and the enantioselectivity (ee) and diastereoselectivity (dr) of homoenolate product are 93% and 17:1, respectively.

3. Results and discussions

3.1 Mechanisms for Path-homo and Path-set

3.1.1 Formation of the Breslow intermediate

As shown in Scheme 2, Path-homo and Path-set first share the same formation process of the Breslow intermediate.[29] It consists of two steps: (1) nucleophilic attack of the original catalyst **5f** to enal **react-1** (2) proton transfer of the formed intermediate **Int1** to yield the Breslow intermediate **Int2**.

*Nucleophilic attack of **5f** to **react-1***

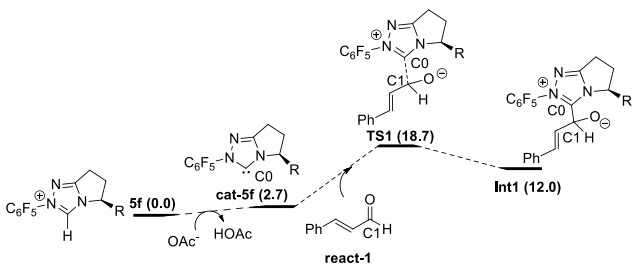

Fig. 1 Nucleophilic attack of **5f** to **react1**

As shown in Fig. 1, with the aid of OAc^- (from base NaOAc), deprotonation[29] of the original catalyst **5f** first occurs to obtain

the active catalyst **cat-5f** and HOAc (the conjugate acid of NaOAc). This process is endergonic by 2.7 kcal/mol. Then **cat-5f** attacks the substrate **react-1** via the C0-C1 forming transition state **TS1** to generate the zwitterionic intermediate **Int1**. The free energy barrier of this step is 18.7 kcal/mol (**5f**+**react1**→**TS1**).

*Proton transfer of **Int1***

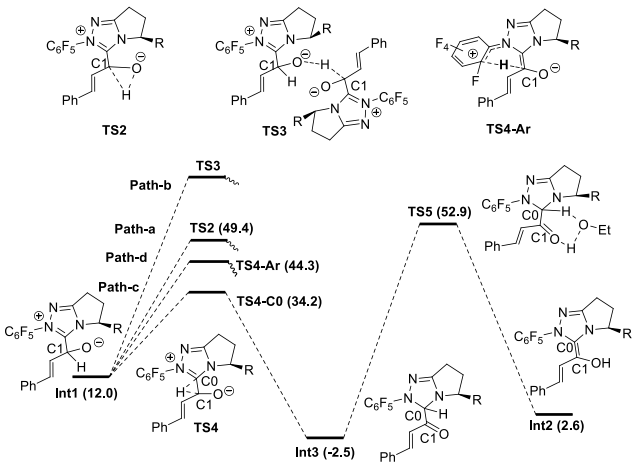

Fig. 2 The mechanisms in the absence of HOAc

Fig. 2 shows the detailed transformations and the energy demands of Path-a, b, c and d. In Path-a, a direct 1,2-proton transfer step occurs via the three-centered transition state **TS2** to generate the Breslow intermediate **Int2**. The energy barrier of this process is 37.4 kcal/mol (**Int1**→**TS2**), and the high energy barrier is in line with the kinetic investigation by White and Leeper.[30] In Path-b, all efforts in locating the transition state (**TS3**) for the intermolecular proton transfer step between two **Int1** molecules were failed. The reason might be related to the high steric hindrance between the two carbene structures, which makes it difficult for the carbonyl oxygen atom of one **Int1** to get close to the C1-H bond of another **Int1**. In Path-c, the indirect hydride transfer from C1 atom to the C0 atom of carbene first occurs via the three-centered transition state **TS4-C0** to generate the intermediate **Int3**. Then with the aid of solvent HOEt, deprotonation of C0 and protonation of O atom occurs simultaneously via the five-centered transition state **TS5** to obtain the Breslow intermediate **Int2**. The energy barrier of Path-c is 40.9 kcal/mol (**Int1**→**TS5**). In Path-d, the hydride transfer from C1 atom to the -C_6F_5 group first occurs via the six-centered transition state **TS4-Ar**. The free energy of this transition state is as high as 44.3 kcal/mol.

From Fig. 2, we found that the Path-a, b, c and d are all unlikely to occur due to the high energy demands and structural limitations.

Fig. 3 shows the detailed transformations and the energy demands of HOAc assisted Path-e and Path-f. In Path-e, the cleavage of C1-H bond and formation of hydroxyl O-H bond are supposed to occur simultaneously in the five-membered ring transition state **TS6** or seven-membered[2b] ring transition state **TS6-O**. However, the elongated C1-H bond always reformed, and both **TS6** and **TS6-O** turned into **Int4** after optimization. In other words, the cleavage of C1-H bond with acid is difficult.The reason might be related to that only partial negative charge was formed on OAc, thus making it difficult to capture the proton of C1-H bond. Indeed, the OAc^- anion directly participated mechanism (Path-f) was found to be much more feasible. As shown in Fig. 3, the O atom of **Int1** is first protonated by HOAc to give the intermediate **Int4** and OAc^-, then **Int4** undergoes OAc^- assisted C1-H cleavage via the transition state **TS7** to give the Breslow intermediate **Int2**. The energy barrier of Path-f is 12.7 kcal/mol (**Int4**→**TS7**).[31]

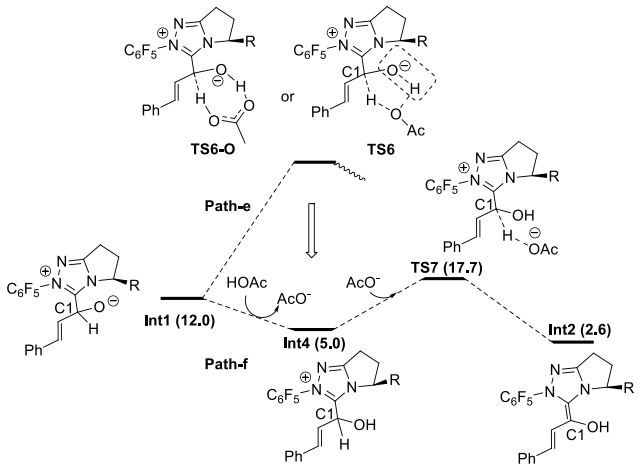

Fig. 3 The mechanisms with the aid of HOAc

From the above calculation results and discussions, it's found that the HOAc mediated stepwise Path-e is energetically more feasible than all the other paths (a, b, c, d and e). In paths a-e, the C1-H cleavage occurs before or simultaneously with O atom protonation, whereas in Path-f protonation of the O atom occurs prior to the C1-H cleavage. The intriguing phenomenon suggests that the C1-H bond cleavage step can be greatly facilitated after the O atom protonation. The reason is understandable, because in **TS7**, the negative charge accumulated on C1 atom during the proton dissociation can be dispersed by the positive charge located on carbene ring. In contrast, the generated negative charge can't be dispersed when it is close to negative charged O atom, thereby destabilizing corresponding transition states (Path a-d). To verify this proposal, the transition state for direct deprotonation of C1-H in the intermediate **Int1** was located (**TS-g** in supporting information[32]). Consistent with our proposal, the relative free energy of **TS-g** is 28.8 kcal/mol higher than that of **Int1**. Therefore, we conclude that the charge dispersion during C1-H bond cleavage process determines the most favourable mechanism (i.e. Path-f).

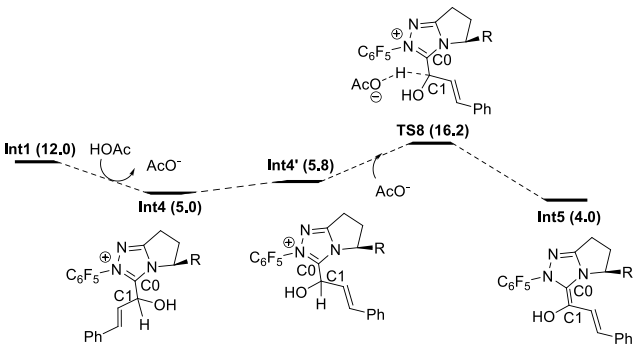

Fig. 4 Proton transfer process to generate **Int5**

Cite this: DOI: 10.1039/c0xx00000x

www.rsc.org/xxxxxx

ARTICLE TYPE

Similar to Path-f, an alternative proton transfer process might occur to generate the isomer of **Int2** (i.e. another Breslow intermediate **Int5**). As shown in Fig. 4, the rotation of the C0-C1 single bond occurs first to generate the intermediate **Int4'**. Then it undergoes OAc^- mediated deprotonation step via **TS8**, and finally results in the formation of **Int5**. According to the calculation results, the energy barrier of the transformation from **Int4** to the Breslow intermediate **Int5** (11.2 kcal/mol) is slightly lower than to **Int2** (12.7 kcal/mol), while the relative Gibbs energy of **Int5** (4.0 kcal/mol) is higher than **Int2** (2.6 kcal/mol).[33]

3.1.2 Subsequent steps of Path-homo

The subsequent process of Path-homo from both Breslow intermediates (**Int5** and **Int2**) is then examined. It consists of three steps: (1) nucleophilic attack of **Int5** and **Int2** to **react-2** in formation of **H-Int6** (2) Protonation of C5 in **H-Int6** to obtain **H-Int9** (3) Enol-keto tautomerisation and attack of OEt to C1 in **H-Int9** to yield homoenolate product.

*Nucleophilic attack of **Int5** and **Int2** to **react-2***

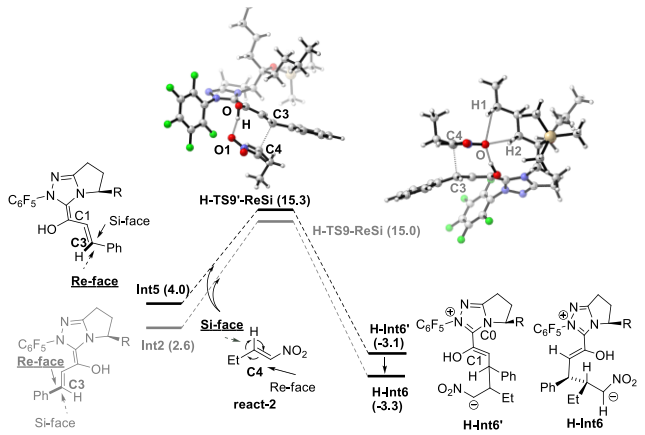

Scheme 5 Nucleophilic attack of **Int5** and **Int2** to **react-2**

As shown in Scheme 5, nucleophilic attack of the C3 atom (in **Int2** and **Int5**) to C4 atom (in **react-2**) might occur via either the Si-face or Re-face, therefore four different modes (3-Si, 4-Si), (3-Si, 4-Re), (3-Re, 4-Si) and (3-Re, 4-Re) are possible in this step. Among these, the (3-Re, 4-Si) attack mode finally leads to the (3S, 4R) configuration product (**prod-homo**) in Rovis's experiment.[12a] As to **Int2**, it occurs via the transition state **H-TS9-ReSi** to directly generate the intermediate **H-Int6** (see supporting information for the other three attack modes). As to **Int5**, it first attacks **react-2** via the transition state **H-TS9'-ReSi** to generate the intermediate **H-Int6'** (see the other three attack modes in section 3.3). Subsequently, **H-Int6'** isomerizes to **H-Int6** via C0-C1 rotation with the energy release of 0.2 kcal/mol. In both of the transition states (**H-TS9-ReSi** and **H-TS9'-ReSi**), hydrogen bond interaction exists between the nitro group and the hydroxyl (In our study, an open transition state in the absence of the intramolecular hydrogen bond was found to be unfavorable. Please see Supporting information for more details). The energy barrier of nucleophilic attack of **Int2** and **Int5** are respectively 12.4 (**Int2→H-TS9-ReSi**) and 11.3 kcal/mol (**Int5→H-TS9'-ReSi**). Additionally, the Breslow inermediate **Int5** is formed preferentially due to a favorable deprotonation transition state (free energy of **TS8** is lower than **TS7**). Note that the C5 atom of **H-Int6** accumulates much negative charge, thus it tends to be protonated in the following step.

*Protonation of C5 in **H-Int6***

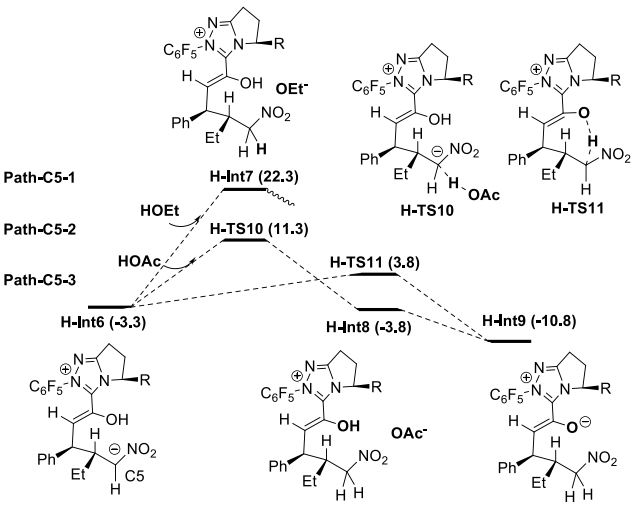

Fig. 5 The energy profiles of protonation processes

Fig. 5 shows three possible protonation mechanisms of C5 in **H-Int6**. Nair et al.[9c] proposed that the C5 atom of **H-Int6** might be directly protonated by the solvent HOEt to give the intermediate **H-Int7** (i.e. Path-C5-1). It is highly endergonic by 25.6 kcal/mol (note: the transition state was failed to be located, and the calculations indicate that such process is continuously endergonic). As mentioned in the introduction, the high energy demand might be attributed to the weak acidity of HOEt, and therefore we investigate the more acidic HOAc participated protonation (i.e. Path-C5-2). From **H-Int6**, HOAc participated protonation occurs via the transition state **H-TS10** to give the intermediate **H-Int8** and OAc^-. The OAc^- anion subsequently captures the proton of hydroxyl in **H-Int8** to generate **H-Int9**. The energy barrier of Path-C5-2 is 14.6 kcal/mol (**H-Int6→H-TS10**) and it is exergonic by 7.5 kcal/mol. Thus, this result seems to suggest that the energy release of hydroxyl deprotonation may compensate the demand of C5 protonation. Thus, we investigate the concerted mechanism (i.e. Path-C5-3). In this mechanism, **H-Int6** undergoes intramolecular protonation via the concerted transition state **H-TS11** to directly obtain intermediate **H-Int9**. As expected, the energy barrier of Path-C5-3 is only 7.1 kcal/mol (**H-Int6→H-TS11**). Therefore, the newly found intramolecular protonation Path-C5-3 is energetically more favorable.

*Enol-keto tautomerisation and attack of OEt to C1 in **H-Int9***

As mentioned in introduction, the obtained intermediate **H-Int9** from the above protonation process undergoes enol-keto tautomerisation (i.e. C2 protonation) and attack of HOEt to C1 to obtain **prod-homo**. The detailed energy profile of this process has been given in Fig. 6 (Path-1).

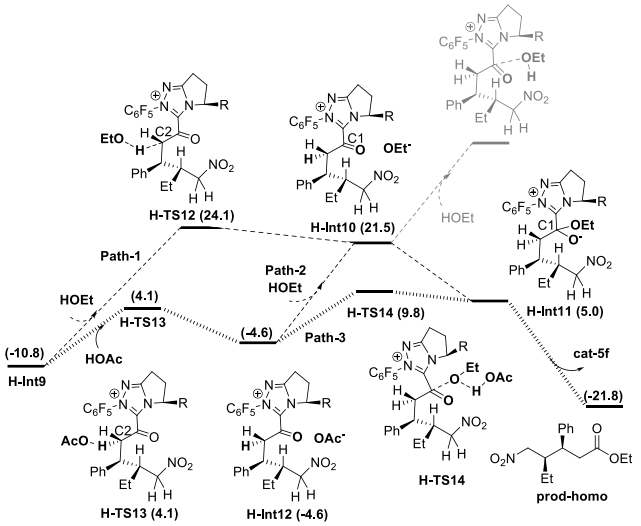

Fig. 6 The energy profiles for paths 1-3

In Path-1, the solvent HOEt first protonates C2 via the transition state **H-TS12** to finish enol-keto tautomerisation. This step generates the intermediate **H-Int10** and OEt^-, with the energy barrier of 34.9 kcal/mol (**H-Int9→H-TS12**) and the energy absorption of 32.3 kcal/mol. Subsequently, the HOEt attackes to C1 of **H-Int10**, ending up with automatic dissociation. Considering that the dissociation of HOEt might be caused by the weak nucleophilicity of HOEt, we take the in situ produced OEt^- to attack the C1 atom to obtain **H-Int11**. It is exergonic by 16.5 kcal/mol. Finally the carbene group dissociates from **H-Int11** to yield **prod-homo**. The energy barrier of Path-1 is 34.9 kcal/mol (**H-Int9→H-TS12**).

As mentioned in Path-C5-1, the weak acidity of HOEt could lead to the high energy demand of protonation (34.9 kcal/mol), we further investigate the more acidic HOAc mediated protonation (Path-2). The intermediate **H-Int9** undergoes HOAc involved C2 protonation via **H-TS13** to generate **H-Int12** and OAc^-. As expected, the energy barrier of this step is only 14.9 kcal/mol. Subsequently, OAc^- captures the proton of HOEt, and the produced OEt^- attacks the C1 atom. This step is endergonic by 16.5 kcal/mol. Thus, the overall energy barrier of Path-2 is 32.3 kcal/mol (**H-Int9→H-Int10**). Although Path-2 is favored over Path-1, the energy barriers of both of them are too high to be satisfied in Rovis's experiment. Thus, we wonder if there is a more plausible mechanism for enol-keto tautomerisation and attack of OEt to C1?

One should note that the direct breakage of H-OEt by OAc^- is highly endergonic while attack of OEt^- to carbonyl is highly exergonic in Path-2. Given this in mind, we tried to investigate Path-3 in which the above two steps occur simultaneously (Fig. 6). From **H-Int12**, OAc^- behaves as a base to capture the H atom of HOEt, meanwhile the OEt group attacks the C1 atom (shown as concerted transition state **H-TS14**). Gratifyingly, the energy barrier of this step is 14.4 kcal/mol (**H-Int12→H-TS14**). Finally, the carbene ring dissociates to give **prod-homo**. Therefore, the overall energy barrier of Path-3 is 20.6 kcal/mol (**H-Int9→H-TS14**), and this HOAc involved enol-keto tautomerisation and concerted attack of OEt to C1 process is the most favored. (See the Supporting Information for another three possible mechanisms Paths 4-6).

3.1.3 The whole process of Path-homo

According to the findings presented above, we gain the following conclusions about Path-homo (Fig. 7). (a) In Breslow intermediate formation process, the HOAc mediated stepwise Path-f is the most favored, due to the good charge dispersion during C1-H bond cleavage process; (b) In protonation process of C5 in **H-Int6**, the newly found intramolecular protonation Path-C5-3 is energetically most favored, because the energy release of hydroxyl deprotonation can recover the demand of the simultaneous C5 protonation; (c) As to enol-keto tautomerisation and attack of OEt to C1 in **H-Int9**, the concerted process Path-3 is operative, since the attack of OEt^- to C1 atom can provide the energy required in the breakage of H-OEt by OAc^-.

Based on these conclusions, the whole process of Path-homo is shown in Fig. 7. It consists of seven steps: (1) nucleophilic attack of NHC to enal, (2) HOAc assisted stepwise proton transfer, (3) nucleophilic attack of Breslow intermediate (C3 atom) to nitroalkene, (4) intramolecular proton transfer (5) HOAc involved protonation of C2, (6) concerted nucleophilic attack of OEt to carbonyl and (7) carbene dissociation. In the second step, there are two different proton transfer transition states **TS8** and **TS7** leading to the Breslow intermediates **Int5** and **Int2**. Since **TS8** is more favorable than **TS7**, the process from **Int4** should be **Int4 →Int5 → H-TS9'-ReSi → H-Int6'→ H-Int6**. The energy barriers of the former six steps are respectively 18.7, 16.2, 15.3, 7.1, 14.9 and 20.6 kcal/mol. The sixth step, i.e. the concerted nucleophilic attack of OEt to carbonyl, is the rate determining step with an overall energy barrier of 20.6 kcal/mol (**H-Int9→H-TS14**).

3.1.4 The whole process of Path-set

Fig. 8 shows the whole process of Path-set. Since Path-homo and Path-set share the same formation process of Breslow intermediates, and become different after them, we investigate subsequent steps of Path-set from the Breslow intermediates **Int5** and **Int2**. As to **Int5**, C1 of this intermediate first attacks C4 in substrate **react-2** to give the intermediate **S-Int12** via (1-Si, 4-Re) mode transition state (**S-TS15-SiRe**).[34] The energy barrier of this step is 15.9 kcal/mol (**5f+react1→S-TS15-SiRe**). Because the C5 atom in **S-Int12** accumulates partial negative charge, it tends to be protonated by intramolecular hydroxyl to generate the intermediate **S-Int13**. The energy barrier is 19.2 kcal/mol (**5f+react1→S-TS16**). The obtained intermediate **S-Int13** finally undergoes rapid carbene dissociation via **S-TS17** to yield Stetter product **prod-set** and the catalyst **cat-5f**. The intramolecular protonation step has the highest energy barrier in the above processes with an energy barrier of 19.2 kcal/mol.

Cite this: DOI: 10.1039/c0xx00000x

www.rsc.org/xxxxxx

ARTICLE TYPE

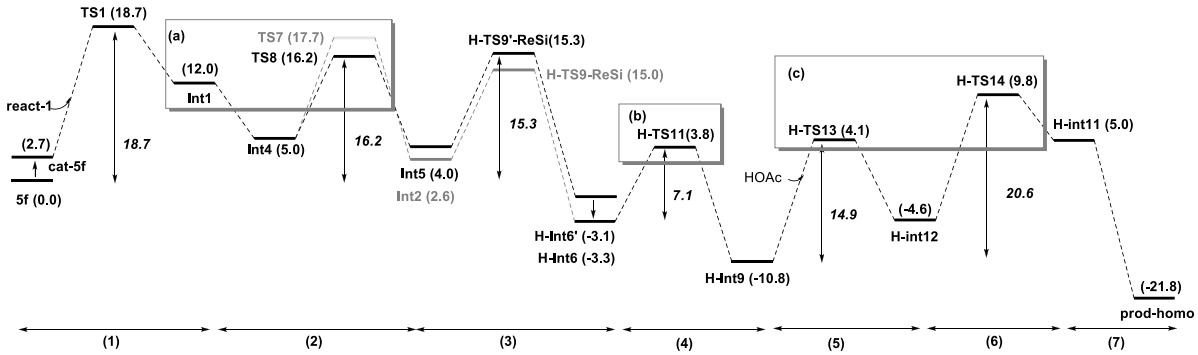

Fig. 7 The whole process of Path-homo

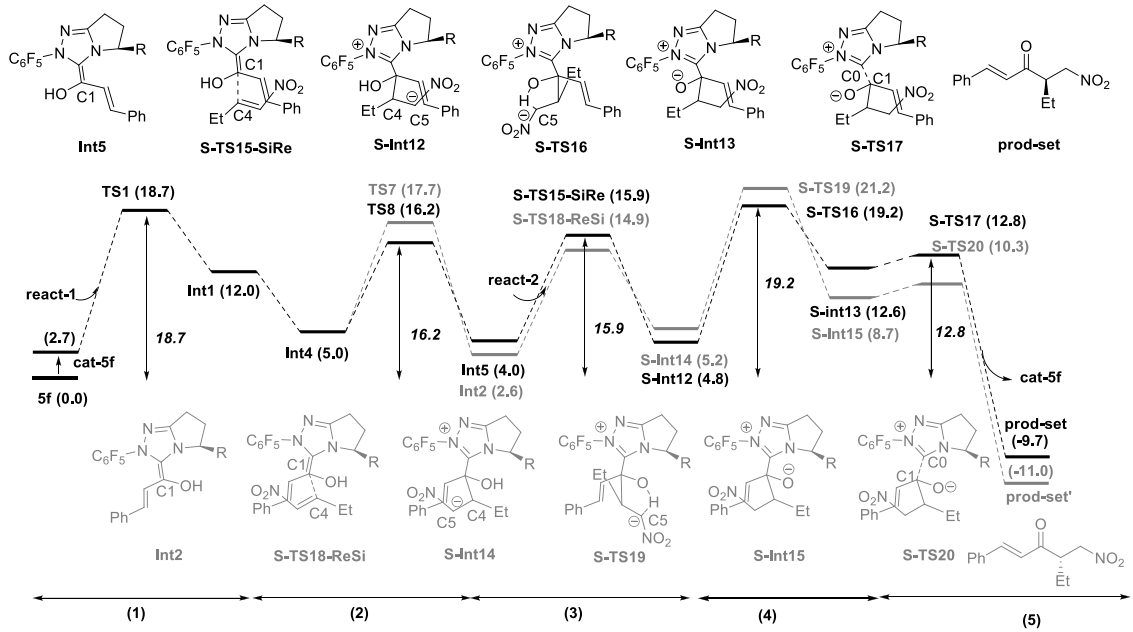

Fig. 8 The whole process of Path-set

Subsequent steps from the Breslow intermediate **Int2** resemble than from **Int5**. First, the Re-face of C1 (in **Int2**) attacks the Si-face of C4 (in substrate **react-2**) with the energy barrier of 14.9 kcal/mol(**5f**+**react1**→**S-TS18-ReSi**).[34] Subsequently, intramolecular protonation occurs with an energy barrier of 21.2 kcal/mol (**5f**+**react1**→**S-TS19**). Finally we obtain product **prod-set'** after rapid carbene dissociation. The intramolecular protonation has the highest energy barrier (21.2 kcal/mol). Thus, the overall energy barriers of the subsequent steps from **Int5** and **Int2** are 19.2 and 21.2 kcal/mol, respectively. Therefore the former is more favourable.

Based on the above results, the whole process of Path-set consists of five steps: (1) nucleophilic attack of NHC to enal, (2) HOAc assisted stepwise proton transfer, (3) nucleophilic attack of Breslow intermediate (C1 atom) to nitroalkene, (4) intramolecular proton transfer and (5) carbene dissociation. The energy barriers of these five steps are 18.7, 16.2, 15.9, 19.2 and 12.8 kcal/mol respectively. The overall energy barrier of Path-set is 19.2 kcal/mol (**cat-5f** + **react1** →**S-TS16**).

3.2 Discussions on chemoselectivity

Cite this: DOI: 10.1039/c0xx00000x

www.rsc.org/xxxxxx

ARTICLE TYPE

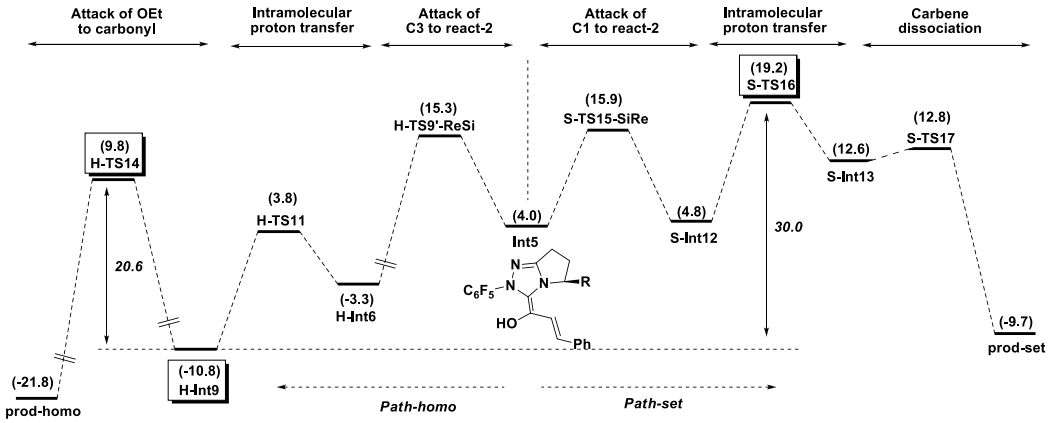

Fig. 9 Comparison between Path-homo and Path-set

Path-homo and Path-set become different from the Breslow intermediate **Int5** (Fig. 9). Herein, we use the energetic span model[35] to compare Path-homo and Path-set. Since **Int5** first undergoes highly exergonic nucleophilic attack step of C3 and kinetically facile intramolecular proton transfer to obtain the most stable intermediate **H-Int9** in the reaction system, this intermediate is the TDI for Path-homo and Path-set. For Path-homo, the attack transition state of OEt to carbonyl (**H-TS14**) is the TDTS, and the related δE is 20.6 kcal/mol. For Path-set, the intramolecular proton transfer transition state **S-TS16** is the TDTS, and the related δE is 30.0 kcal/mol. Therefore, δE of Path-homo is smaller than that of Path-set, and Path-homo has larger TOF. In addition, the product of Path-homo (**prod-homo**) is thermodynamically more stable than the product of Path-set (**prod-set**). Therefore, Path-homo is kinetically and thermodynamically more favored than Path-set, and this conclusion consists with Rovis's experiment[12a] where homoenolate product was obtained predominantly. Furthermore, the highly exergonic nucleophilic attack (i.e. the thermodynamic stability of **H-Int6**) and the facile subsequent steps (intramolecular proton transfer and attack of OEt to carbonyl) in path-homo result in the feasibility of the homoenolate reaction.

3.3 Discussions on stereoselectivity of Path-homo

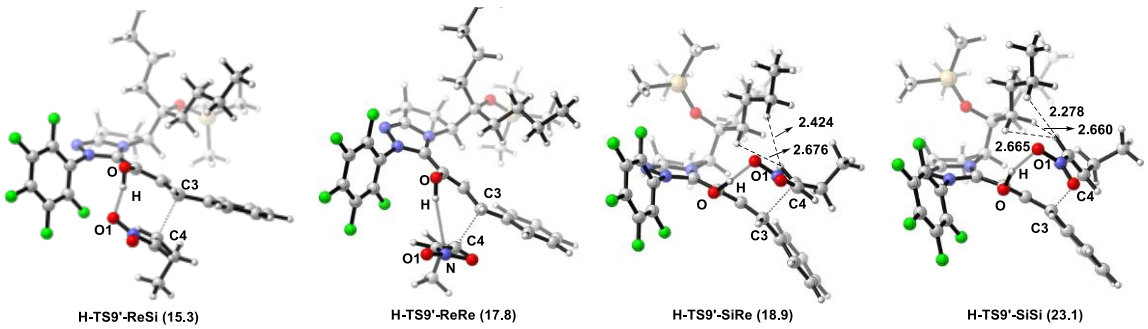

Fig. 10 Transition states for nucleophilic attack of **Int5** to **react-2**

The nucleophilic attack of Breslow intermediate **Int5** to nitroalkene **react-2** determines the stereoselectivity of Path-homo. As shown in Fig. 10, four different attack modes (3-Re, 4-Si), (3-Re, 4-Re), (3-Si, 4-Re) and (3-Si, 4-Si) are possible in this step. Their corresponding transition states are **H-TS9'-ReSi**, **H-TS9'-ReRe**, **H-TS9'-SiRe** and **H-TS9'-SiSi**, and they finally lead to (3S, 4R) (3S, 4S) (3R, 4S) and (3R, 4R) configuration products. The Gibbs free energies of these four transition states are 15.3, 17.8, 18.9 and 23.1 kcal/mol, respectively. Therefore, (3-Re, 4-Si) attack mode leading to the *syn*-configuration product (**prod-homo**) is the most favourable mechanism. The second favourable attack mode (3-Re, 4-Re) leads to *anti*-configuration product. The calculation results consist well with the unexpectedly obtained *syn* configuration product in Rovis's experiment.[12a]

Structural observations on the former two transition states (**H-TS9'-ReSi** and **H-TS9'-ReRe**) show that C4 plane is below the C3 plane (Fig. 10). Therefore, the Et group of substrate **react-2** is far away from alkyl substituent (i.e. R) on the carbene ring, and little steric effect exists between them. In addition, the former transition state is more favored than the latter, because of a larger

hydrogen bonding interaction exists between O-H···O1 in the former case (the bond distances are 1.656 Å and 3.099 Å in **H-TS9'-ReSi** and **H-TS9'-ReRe**). In contrast, in the latter two transition states (**H-TS9'-SiRe** and **H-TS9'-SiSi**), large steric effects exist between -Et and -nBu of R group reflected by H···H interactions (bond length of H1···H2 and H1···H3 in **H-TS9'-SiRe** are 2.424Å and 2.676Å, meanwhile they are 2.278Å and 2.665Å in **H-TS9'-SiSi**) [36].

Based on the aforementioned discussions, we propose that the less steric hindrance between Et and nBu, and stronger hydrogen bonding interaction between O-H···O1 in **H-TS9'-ReSi** result in the observed *syn* stereoselectivity.

4. Conclusion

Recently, Rovis group reported a homoenolate reaction between alkyl substituted nitroalkenes and enals, obtaining *syn* configuration product accompanied with trace amount of Stetter reaction byproduct. In the present study, we carried out DFT calculations to investigate the detailed mechanism of nitroalkene participated homoenolate reaction, and explain the origin of the homoenolate chemoselectivity and *syn* stereoselectivity. Our calculations indicate that: Path-homo and Path-set first share the same formation process of Breslow intermediates. It proceeds via HOAc mediated stepwise Path-f (rather than Path-a to e), due to the good charge dispersion during C1-H bond cleavage process. Subsquent process of Path-homo consists of five steps: nucleophilic attack of Breslow intermediate (C3 atom) to nitroalkene; intramolecular proton transfer (rather than HOEt or HOAc mediated stepwise mechanism, because the energy release of hydroxyl deprotonation can recover the demand of the C5 protonation); HOAc involved protonation of C2; concerted nucleophilic attack of OEt to carbonyl (instead of HOEt or HOAc involved stepwise mechanism, since attack of OEt^- to carbonyl can provide the energy required in the breakage of H-OEt by OAc^-); and final carbene dissociation. Subsquent process of Path-set consists of three steps: nucleophilic attack of Breslow intermediate (C1 atom) to nitroalkene, intramolecular proton transfer and carbene dissociation. Path-homo is found to be more feasible than Path-set. The thermodynamic stability of the **H-int6** and the facile intramolecular proton transfer and attack of OEt to carbonyl in Path-homo result in its feasibility. Furthermore, the stereoselective determining step of Path-homo is the attack of Breslow intermediate to the nitroalkene, in which the steric hindrance and hydrogen bonding determine the *syn* stereoselectivity.

Acknowledgement

We thank the NSFC (21172209, 21272223, 21202006), SRFDP(20123402110051), FRFCU (WK2060190025, FRF-TP-13-023A),CAS (KJCX2-EW-J02), Fok Ying Tung Education Foundation, ChinaGrid project funded by MOE of China, and the supercomputer center of Shanghai and USTC.

Notes and references

[a] *Department of Chemistry, University of Science and Technology of China, Hefei,230026, China. E-mail: fuyao@ustc.edu.cn; Fax: (+86)-551-360-6689;Tel: (+86)-551-360-7476*

[b] *Department of Polymer Science and Engineering, University of Science and Technology Beijing, Beijing 100083, PR China*

† Electronic Supplementary Information (ESI) available: [The complete contents for refs 31-34, and Cartesian coordinates, free energies, and thermal corrections.]. See DOI: 10.1039/b000000x/

‡ Footnotes should appear here. These might include comments relevant to but not central to the matter under discussion, limited experimental and spectral data, and crystallographic data.

1 (a) D. Enders, O. Niemeier, A. Hensler, *Chem. Rev.*, 2007, **107**, 5606; (b) V. Nair, S. Vellalath, B. P. Babu, *Chem. Soc. Rev.*, 2008, **37**, 2691; (c) J. Read de Alaniz, T. Rovis, *Synlett*, 2009, 1189; (d) H. U. Vora, T. Rovis, *Aldrichimica Acta*, 2011, **44**, 3; (e) X. Bugaut, F. Glorius, *Chem. Soc. Rev.*, 2012, **41**, 3511; (f) N. Marion, S. Díez-González, S. P. Nolan, *Angew. Chem., Int. Ed.*, 2007, **46**, 2988; (g) E. M. Phillips, A. Chan, K. A. Scheidt, *Aldrichimica Acta*, 2009, **42**, 55; (h) J. L. Moore, T. Rovis, *Top Curr. Chem.*, 2010, **291**,77; (i) P. C. Chiang, J. W. Bode, *TCI Mail*, 2011, **149**, 2; (j) A. T. Biju, N. Kuhl, F. Glorius, *Acc. Chem. Res.*, 2011, **44**, 1182.

2 (a) H. Stetter, H. Kuhlmann, in Org. React., ed. L. A. Paquette, Wiley, New York, 1991, vol. 40, pp. 407–496; (b) D. A. DiRocco, T. Rovis, *J. Am. Chem. Soc.* 2011, **133**, 10402; (c) D. A. DiRocco, K. M. Oberg, D. M. Dalton, T. Rovis, *J. Am. Chem. Soc.* 2009, **131**, 10872; (d) M. S. Kerr, J. Read de Alaniz, T. Rovis, *J. Am. Chem. Soc.* 2002, **124**, 10298; (e) Q. Liu, S. Perreault, T. Rovis, *J. Am. Chem. Soc.* 2008, **130**, 14066.

3 (a) D. Enders, K. Breuer, G. Raabe, J. Runsink, J. H. Teles, J. P. Melder, K. Ebel, S. Brode, *Angew. Chem., Int. Ed. Engl.*,1995, **34**, 1021; (b) D. Enders, K. Breuer, J. H. Teles, *Helv. Chim. Acta*, 1996, **79**, 1217; (c) D. Enders, U. Kallfass, *Angew. Chem., Int. Ed.*, 2002, **41**, 1743; (d) R. L. Knight, F. J. Leeper, *J. Chem. Soc., Perkin Trans*. 1998, **1**, 1891.

4 Z. Q. Rong, W. Zhang, G. Q. Yang and S. L. You, *Curr. Org. Chem.*, 2011, **15**, 3077.

5 (a) S. P. Lathrop, T. Rovis, *J. Am. Chem. Soc.*, 2009, **131**, 13628; (b) C. M. Filloux, S. P. Lathrop, T. Rovis, *Proc. Natl. Acad. Sci. U.S.A.*, 2010, **107**, 20666; (c) G. L. Zhao, A. Córdova, *Tetrahedron Lett.*, 2007, **48**, 5976; (d) H. Jiang, B. Gschwend, L. Albrecht, K. A. Jørgensen, *Org. Lett.*,2010, **12**, 5052.

6 V. Nair, R. S. Menon, A. T. Biju, C. R. Sinu, R. R. Paul, A. Jose, V. Sreekumar, *Chem. Soc. Rev.*, 2011, **40**,5336.

7 (a) S. S. Sohn, E. L. Rosen, J. W. Bode, *J. Am. Chem. Soc.*, 2004, **126**, 14370; (b) M. He, J. W. Bode, *Org. Lett.*, 2005, **7**, 3131; (c) P. C. Chiang, J. Kaeobamrung, J. W. Bode, *J. Am. Chem. Soc.*, 2007, **129**, 3520; (d) M. Rommel, T. Fukuzumi, J. W. Bode, *J. Am. Chem. Soc.*, 2008, **130**, 17266.

8 C. Burstein, F. Glorius, *Angew. Chem., Int. Ed.*, 2004, **43**, 6205.

9 (a) V. Nair, S. Vellalath, M. Poonoth, E. Suresh, *J. Am. Chem. Soc.*, 2006, **128**, 8736; (b) V. Nair, M. Poonoth, S. Vellalath, E. Suresh, R. Thirumalai, *J. Org. Chem.*, 2006, **71**, 8964; (c) V. Nair, C. R. Sinu, B. P. Babu, V. Varghese, A. Jose, E. Suresh, *Org. Lett*., 2009, **11**, 5570; (d) V. Nair, B. P. Babu, S. Vellalatha, E. Suresh, *Chem. Commun*, 2008,747.

10 (a) E. M. Phillips, T. E. Reynolds, K. A. Scheidt, *J. Am. Chem. Soc.*, 2008, **130**, 2416; (b) B. C. David, D. E. A. Raup, K. A. Scheidt, *J. Am. Chem. Soc.*, 2010, **132**, 5345; (c) J. Izquierdo, A. Orue, K. A. Scheidt, *J. Am. Chem. Soc.*, 2013, **135**, 10634; (d) D. T. Cohen, B. C. David, K. A. Scheidt, *Angew. Chem., Int. Ed.*, 2011, **50**, 1678; (e) M. Wadamoto, E. M. Phillips, T. E. Reynolds, K. A. Scheidt, *J. Am. Chem. Soc*., 2007, **129**, 10098.

11 B. Maji, L. Ji, S.Wang, S. Vedachalam, R. Ganguly, X. W. Liu, *Angew. Chem., Int. Ed.*, 2012, **51**, 8276.

12 (a) N. A. White, D. A. DiRocco, T. Rovis, *J. Am. Chem. Soc.*,2013, **135**, 8504; (b) X. Zhao, D. A. DiRocco, T. Rovis, *J. Am. Chem. Soc.*, 2011, **133**, 12466.

13 Mechanism studies of Stetter reaction: (a) J. L. Moore, A. P. Silvestri, J. Read de Alaniz, D. A. DiRocco, T. Rovis, *Org. Lett.*, 2011, **13**, 1742; (b) J. M. Um, D. A. DiRocco, E. L. Noey, T. Rovis, K. N. Houk, *J. Am. Chem. Soc.*, 2011, **133**, 11249; (c) D. A. DiRocco, E. L. Noey, K. N. Houk, T. Rovis, *Angew. Chem. Int. Ed.*, 2012, **51**, 2391.

14 (a) J. Martí, F. Lopez-Calahorra, J. M. Bofill, *Theochem*, 1995, **339**, 179; (b) F. Lopez-Calahorra, J. Castells, L. Doming, J. Martí, J. M. Bofill, *Heterocycles*.,1994, **37**, 1579.

15 K. J. Hawkes, B. F. Yates, *Eur. J. Org. Chem.*, 2008, 5563.

16 P. Verma, P. A. Patni, R. B. Sunoj, *J. Org. Chem.*, 2011, **76**, 5606.

17 L. R. Domingo, M. J. Aurell, M. Arnó, *Tetrahedron*, 2009,**65**, 3432.

18 Y. Q. He, Y. Xue, *J. Phys. Chem. A*, 2011, **115**, 1408.

19 C. J. Collett, R. S. Massey, O. R. Maguire, A. S. Batsanov, A. C. O'Donoghue, A. D. Smith, *Chem. Sci.*, 2013, **4**, 1514.

20 J.-S. Zheng, H.-N. Chang, F.-L. Wang, L. Liu, *J. Am. Chem. Soc.* 2011, **133**, 11080.

21 M. J. Frisch, G. W. Trucks, H. B. Schlegel, G. E. Scuseria, M. A. Robb, J. R. Cheeseman, G. Scalmani, V. Barone, B. Mennucci, G. A. Petersson, H. Nakatsuji, M. Caricato, X. Li, H. P. Hratchian, A. F. Izmaylov, J. Bloino, G. Zheng, J. L. Sonnenberg, M. Hada, M. Ehara, K. Toyota, R. Fukuda, J. Hasegawa, M. Ishida, T. Nakajima, Y. Honda, O. Kitao,H. Nakai, T. Vreven, J. A. Montgomery, Jr., J. E. Peralta, F. Ogliaro, M. Bearpark, J. J. Heyd, E. Brothers, K. N. Kudin, V. N. Staroverov, R. Kobayashi, J. Normand,K. Raghavachari, A. Rendell, J. C. Burant, S. S. Iyengar,J. Tomasi, M. Cossi, N. Rega, J. M. Millam, M. Klene, J. E. Knox, J. B. Cross, V. Bakken, C. Adamo, J. Jaramillo, R. Gomperts, R. E. Stratmann, O. Yazyev, A. J. Austin, R. Cammi, C. Pomelli, J. W. Ochterski, R. L. Martin, K. Morokuma, V. G. Zakrzewski, G. A. Voth, P. Salvador, J. J. Dannenberg, S. Dapprich, A. D. Daniels, Ö. Farkas, J. B. Foresman, J. V. Ortiz, J. Cioslowski and D. J. Fox, *GAUSSIAN 09 (Revision B.01)*, Gaussian Inc., Wallingford CT, 2009.

22 (a) A. D. Becke, *J. Chem. Phys.*, 1993, **98**, 5648; (b) C. Lee, W. Yang, R. G. Parr, *Phys. Rev. B*,1988, **37**, 785.

23 The DFT method B3LYP has been used in many theoretical studies for organic reaction systems: (a) Y. Feng, L. Liu, J.-T. Wang, S.-W. Zhao, Q.-X. Guo, *J. Org. Chem.* 2004, **69**, 3129; (b) Y. Q. He, Y Xue, *J. Phys. Chem. A*, 2010, **114**, 9222; (c) R. Shang, Q. Xu, Y.-Y. Jiang, Y. Wang, L. Liu, *Org. Lett.* 2010, **12**, 1000; (d) Q. Zhang, H. Z. Yu, J. Shi, *Acta Phys.-Chim. Sin.*, 2013, **29**, 2321; (e) C. Wang, L. Liu, *Chin. J. Chem.* 2012, **30**, 1974; (f) M. N. Paddon-Row, C. D. Anderson, K. N. Houk, *J. Org. Chem.*, 2009, **74**, 861; (g) A. E. Hayden, K. N. Houk, *J. Am. Chem. Soc.*, 2009, **131**, 4084.

24 A. W. Ehlers, M. Bohme, S. Dapprich, A. Gobbi, A. Hollwarth, V. Jonas, K. F. Kohler, R. Stegmman, A. Veldkamp, G. Frenking, *Chem. Phys. Lett.*,1993, **208**, 111.

25 (a) H. Z. Yu, D. J. Liu, Z. M. Dang, D. R. Wang, Y. Fu, *Chin. J. Chem.* 2013, **31**, 200; (b) M. S. T. Morin, D. J. St-Cyr, B. A. Arndtsen, E. H. Krenske, K. N. Houk, *J. Am. Chem. Soc.*, 2013, **135**,17349; (c) Q. L. Xu, H. Gao, M. Yousufuddin, D. H. Ess, L. Kürti, *J. Am. Chem. Soc.*, 2013, **135,** 14048; (d) R. Shang, Z.-W. Yang, Y. Wang, S.-L. Zhang, L. Liu, *J. Am. Chem. Soc*. 2010, **132**, 14391; (e) A. Adhikary, A. Kumar, B. J. Palmer, A. D. Todd, M. D. Sevilla, *J. Am. Chem. Soc.*, 2013, **135**, 12827

26 A. Hollwarth, M. Bohme, S. Dapprich, A. W. Ehlers, A. Gobbi, V. Jonas, K. F. Kohler, R. Stegmann, A. Veldkamp, G. Frenking, *Chem. Phys. Lett.*, 1993, **208**, 237.

27 Y. Zhao, D. G. Truhlar, *Theor. Chem. Acc.*, 2008, **120**, 215.

28 The M06 method has been used in many metal free systems for single-point energy calculations: (a) J. M. Lee, P. Helquist, O. Wiest, *J. Am. Chem. Soc.*, 2012, **134**, 14973; (b) O. L. Griffith, J. E. Anthony, A. G. Jones, Y. Shu, D. L. Lichtenberger, *J. Am. Chem. Soc.*, 2012, **134**, 14185; (c) Y. Chen, M. T. Rodgers, *J. Am. Chem. Soc.*, 2012, **134**, 5863; (d) Y. Chen, M. T. Rodgers, *J. Am. Chem. Soc.*, 2012, **134**, 2313.

29 (a) R. Breslow, *J. Am. Chem. Soc.*, 1958, **80**, 3719; (b) A. Lapworth, *J. Chem. Soc.*, 1903, **83**, 995; (c) H. Z. Yu, Y. Fu, L. Liu, Q.-X. Guo, *Chin. J. Org. Chem.* 2007, **27**, 545.

30 M. J. White, F. J. Leeper, *J. Org. Chem.*, 2001, **66**, 5124.

31 We took the proton transfer step (Path-f) as an example to investigate the influence of hydrogen bonding, and it turned out that hydrogen bonding induced by solvent is unlikely to occur. Please see Supporting information for details.

32 Mechanism Path-g was also examined in which C1-H bond of **Int1** break first via **TS-g**. See the Supporting Information for more details.

33 We have investigated the formation of the diastereomer of **Int1** and the transition states for conversion of both diastereomers into **Int2** and **Int5**. Detailed results are given in the Supporting Information.

34 Other three attack mode (1-Si, 4-Si), (1-Re, 4-Re), (1-Re, 4-Si) of **Int5**, and another three attack mode (1-Si, 4-Si), (1-Re, 4-Re), (1-Si, 4-Re) of **Int2** in stetter reaction are placed in Supporting Information.

35 (a) S. Kozuch, S. Shaik, *Acc. Chem. Res.*, 2011, **44**, 101; (b) Z. Li, C. Wang, Y. Fu, Q.-X. Guo, L. Liu, *J. Org. Chem.* 2008, **73**, 6127; (c) C. Wang, Y. Fu, Q.-X. Guo, L. Liu, *Chem. Eur. J.* 2010, **16**, 2586; (d) S.-L. Zhang, Y. Fu, R. Shang, Q.-X. Guo, L. Liu, *J. Am. Chem. Soc.* 2010, **132**, 638; (e) Y.Y. Jiang, H. Z. Yu, Y. Fu, *Organometallics*, 2013, **32**, 926.

36 (a) X. Hong, P. Liu, K. N. Houk, *J. Am. Chem. Soc.*, 2013, **135**, 1456; (b) A. Patel, G. A. Barcan,O. Kwon, K. N. Houk, *J. Am. Chem. Soc.*, 2013, **135**, 4878.

Journal Name

Organic Chemistry Frontiers

Dynamic Article Links ►

Cite this: DOI: 10.1039/c0xx00000x

www.rsc.org/xxxxxx

ARTICLE TYPE

Entry for the Table of Contents

Computational Chemistry

*Qi Zhang, Hai-Zhu Yu, Yao Fu**

Page – Page

NHC-Catalyzed Homoenolate Reaction of Enals and Nitroalkenes: Computational Study of Mechanism, Chemoselectivity and Stereoselectivity

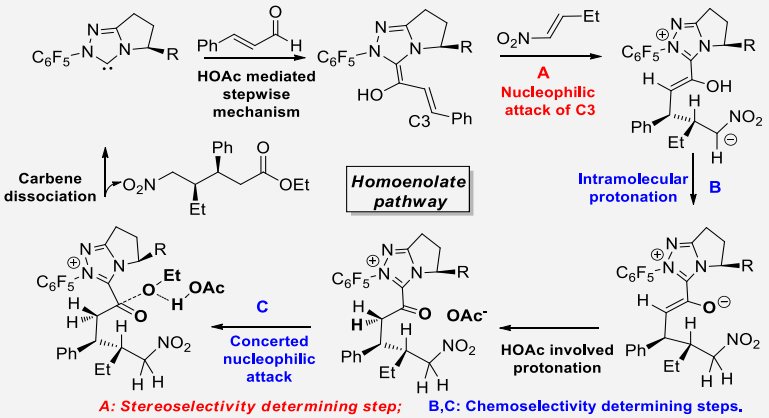

Mechanistic study on NHC-catalyzed homoenolate reaction of enals and nitroalkenes has been performed with DFT calculations.